



Seismic design and analysis of a medium-density residential building

C. Gribbon, Z. Jennings, T. J. Sullivan & G. De Francesco

University of Canterbury, Christchurch.

ABSTRACT

There is an increasing recognition that good seismic performance requires not only checks on life-safety but also limitation of damage, disruption and losses. In light of this, several proposals are currently being developed for alternative seismic design criteria. In this research, the seismic performance of a four-storey residential building in Wellington with reinforced concrete (RC) walls, designed first using the current New Zealand Standards and then low damage design criteria, is assessed using the FEMA P-58 Performance-Based Earthquake Engineering (PBEE) framework. As part of this procedure, accurate non-linear models of the case study buildings were developed in RUAUMOKO3D to determine the probable floor accelerations and drifts. Loss assessment was undertaken using fragility and consequence functions, with reference to New Zealand functions where possible. Comparing the loss estimates obtained for the different designs, it is concluded that the low damage criteria should lead to a significant reduction in losses, and hence improved seismic performance.

1 INTRODUCTION

Multi-storey buildings are commonly designed to prioritise life-safety. As shown by the performance observed during the 2010-2011 Canterbury sequence and 2016 Kaikoura earthquakes, seismic performance should also be quantified in terms of losses. An effective design should provide life-safety while minimising monetary losses and disruption. Minimising expected losses associated with seismic damage is important to all stakeholders due to the adverse monetary and downtime impact. Low damage seismic design (LDSD) criteria currently are under development to provide engineers with a guideline to minimise the loss (Campbell, 2018). This paper investigates how design according to current New Zealand standards (code-compliant) and low damage seismic design affects the losses caused by earthquakes of different return periods based on a four-storey medium density RC residential building in Wellington.

2 METHODOLOGY

The initial structural analysis for the code-compliant design was performed on the case study building using the equivalent static force-based design method (Standards New Zealand, 2004a). The force-based approach

was utilised to provide preliminary sizing and reinforcement details of the RC structural walls. A modal response spectrum analysis was undertaken within SAP2000 to account for the higher mode and torsional effects.

The LDSO approach was undertaken to compare the expected inter-storey drifts, floor accelerations and annual losses to the code-compliant design. The LDSO guidelines consist of damage control limit state (DCLS) criteria and method of direct assessment of a structure. The low damage system was designed using criteria which included a (i) maximum ductility factor for the primary structure, (ii) a limit of six stories, (iii) no vertical or plan irregularity, (iv) element lateral load limitations, and (v) inter-storey deflection limits for the DCLS design actions.

The computer program RUAUMOKO3D (Carr, 2004), developed at University of Canterbury, was used to produce a piece-wise non-linear time history analysis of the buildings. The analysis was conducted to determine the expected inter-storey drifts and floor accelerations from 180 earthquake records (Yeow et al., 2018). The results from the non-linear time history analysis were used to undertake a loss assessment using fragility and consequence functions, with reference to New Zealand functions (Yeow et al., 2018).

3 CASE STUDY BUILDING DESIGN



Figure 1: Elevation view of case study medium density residential building (Carradine, 2019).

The case study building is based on a 2014 architectural concept four-storey apartment building presented in section 10 of the multi-storey light timber framed buildings in New Zealand document (Fig. 1) (Carradine, 2019).

The provided case study building structural system was designed using RC structural walls for the lateral resisting system and steel-framed structure for the gravity system. The code compliant structural system was designed to avoid major clashes with architectural elements (Fig. 2).

The LDSO of the building was refined in SAP2000. The wall sections were increased and relocated to provide additional lateral restraint, minimise the torsional effects and reduce inter-storey drift. Certain architectural restrictions of the building in the Y-direction were neglected to permit satisfaction of LDSO requirements (Fig. 3).

The LDSO of the building was refined in SAP2000.



Figure 2: RC wall layout for Wellington case study building for code compliant design (Carradine, 2019).



Figure 3: RC wall layout for Wellington case study building for LDSO (Carradine, 2019).

SAP2000 was used to conduct a modal response spectrum analysis of the code compliant and LDSD structural layouts. The RC walls were modelled as cantilever beam elements and the gravity structure as steel beams and columns. The structural components were modelled using preliminary sizing demands and capacities. Each storey was constrained as a rigid diaphragm in the X and Y direction. This distributes all seismic forces through the rigid diaphragm and to the structural walls acting as the sole lateral restraint system. The gravity structure was modelled with pinned connections to ensure all seismic actions are carried by the structural walls. The structural layouts for the code-compliant design and LDSD are shown in Figure 4.

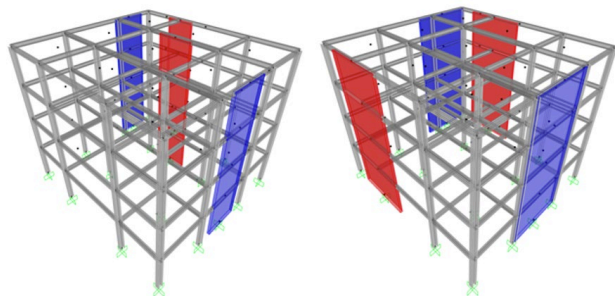


Figure 4: SAP2000 model of building for code compliant design (left) and low damage design (right)

The response spectra for each building design was defined as per NZS1170.5 and input as a function in SAP2000. The response spectrum for a 500 year return period was used to find the force demands on both structures and the ULS inter-storey drift for the code-compliant design. The 250 year return period spectra was used to determine the inter-storey drift demands for the LDSD system. The scale factor for the response spectrum was determined based on the change in ductility as specified in Section 3.2 of this report. The demands from the SAP2000 response spectrum analysis were used to undergo the design of reinforcement for each wall.

3.1 Design assumptions

The response spectra were determined for the Wellington site using a hazard factor of 0.4, soil type C, with a near-fault factor of 1.3. The return period factors for ULS, DCLS and SLS were taken as 1.0, 0.75 and 0.25, respectively. An assumed ductility of 3.0 and 2.0 for the code-compliant design and low damage design, respectively. The seismic mass of the structure was estimated using preliminary gravity structure section sizes, a composite floor system, and previously designed wall sections. The dead and live loads were determined as per NZS1170.1 (Standards New Zealand, 2002) (Table 1).

Table 1: Case study seismic mass components.

| | Measure | Weight/Floor | kPa |
|--------------|--------------------|----------------------|------------|
| Columns | 96 m | 158 kg/m | 0.2 |
| Beams | 416 m | 53.7 kg/m | 0.3 |
| Walls | 264 m ² | 24 kg/m ³ | 1.9 |
| Floor | 720 m ² | 3.0 kPa | 3.0 |
| Dead* | 720 m ² | 1.5kPa | 1.5 |
| Live | 720 m ² | 1.5 kPa | 0.4** |
| Total | - | - | 7.3 |

* including SIDL

** 0.3 seismic mass reduction

properties (Standards New Zealand, 2006). Shear reinforcement design has not been undertaken as part of this research as this was not necessary for the development of non-linear time-history analysis models. The shear capacity was assumed to be sufficient for all walls.

The seismic weight of the building was simplified by applying 9 evenly distributed weights across each floor plan to account for the torsional effects on the building. The architectural layout of the building was simplified to a regular four-storey building, altering the penthouse duplex to a 3.0 m top storey as per the lower floors. The floor was modelled in SAP2000 as a diaphragm to distribute all lateral loads to the RC structural walls. The gravity system was assumed to take no lateral loads. The RC structural walls have been modelled in SAP2000 using 30% of the modulus of elasticity of 40MPa concrete to account for the cracked section

3.2 Critical design criteria

The inter-storey ULS drift limit of 2.5% as defined in NZS1170.5 does not tend to be critical for a RC wall structure due to its high stiffness. Thus, the critical design criteria for the code-compliant wall design was the ULS moment demand. The longitudinal reinforcement was designed for the ULS moment demand and a maximum reinforcement ratio of 1.26% was obtained (Table 4). The peak inter-storey drift for the code-compliant design was less than 50% of the drift limit (Table 3) and the ULS moment demand-capacity ratio (DCR) was up to 95% (Table 2). The DCLS inter-storey drift limit of 0.5% for a 250 year return period was critical in the design of the RC walls for the low damage design building. This determined the required section dimensions of each wall. The drift demand reached 78% of the DCLS drift limit. Repositioning of the walls was undertaken to minimise torsional rotation. The reinforcement was specified after the drift was limited to 0.5%. The longitudinal reinforcement of the LDSD walls have been designed to a maximum bending DCR of 96% (Table 2).

3.3 Design results

The SAP2000 response spectrum analysis determined the design moment acting on the structural walls. The wall section and reinforcement details were designed to be sufficient for the demands obtained from the ULS response spectrum analysis of the code-compliant design and LDSD (Table 2). Inter-storey drifts from the response spectrum analysis were checked against NZS1170.5 drift limits and DCLS limits (Table 3).

Table 2: ULS bending demand and capacity of RC walls for code compliant design and LDSD.

| | | Bending demand (kN-m) | Bending capacity (kN-m) | Ratio |
|--------------|----|-----------------------|-------------------------|-------|
| Code (1/500) | X1 | 3820 | 4036 | 94.6% |
| | X2 | 3700 | 4053 | 91.3% |
| | Y1 | 4470 | 4917 | 90.9% |
| | Y2 | 1775 | 1892 | 93.8% |
| LDSD (1/500) | X1 | 11576 | 12664 | 91.4% |
| | X2 | 11444 | 12693 | 90.2% |
| | Y1 | 12330 | 12839 | 96.0% |
| | Y2 | 12280 | 12839 | 95.6% |

Table 3: Inter-storey drift results for code-compliant design ($\mu=1$, AEP=1/500) and LDSD ($\mu=1$, AEP=1/250)

| | | Inter-storey drift (%) | Inter-storey drift limit (%) | DCR |
|--------------|---|------------------------|------------------------------|-------|
| Code (1/500) | X | 0.89% | 2.50% | 35.6% |
| | Y | 1.22% | 2.50% | 48.8% |
| LDSD (1/250) | X | 0.35% | 0.50% | 70.0% |
| | Y | 0.39% | 0.50% | 78.0% |

The corresponding reinforcement ratios and wall sections for code compliant design and LDSD are detailed in Table 4 and Table 5, respectively. The ULS demands determined by the response spectrum analysis allowed for the design of the longitudinal reinforcement (Standards New Zealand, 2006). The LDSD used the non-torsional wall layout with equal wall sections to ensure equal lateral load resistance. The wall section, demands and reinforcement details obtained from the ULS response spectrum analysis of the LDSD design are shown in Table 5.

Table 4: ULS design for code-compliant building ($\mu=3$, AEP=1/500).

Table 5: ULS design for LDSD building ($\mu=2$, AEP=1/500).

| | X1 | X2 | Y1 | Y2 |
|-------------------------|------|------|------|------|
| Period (s) | 0.46 | | 0.55 | |
| Wall Thickness (m) | 0.2 | 0.2 | 0.25 | 0.2 |
| Wall Length (m) | 3.0 | 3.0 | 3.0 | 2.5 |
| Base Moment (kN-m) | 3820 | 3700 | 4470 | 1775 |
| Reinforcement Ratio (%) | 1.26 | 1.26 | 1.01 | 0.80 |

| | X1 | X2 | Y1 | Y2 |
|-------------------------|-------|-------|-------|-------|
| Period (s) | 0.34 | | 0.32 | |
| Wall Thickness (m) | 0.2 | 0.2 | 0.2 | 0.2 |
| Wall Length (m) | 5.0 | 5.0 | 5.0 | 5.0 |
| Base Moment (kN-m) | 11580 | 11440 | 12330 | 12280 |
| Reinforcement Ratio (%) | 1.51 | 1.51 | 1.51 | 1.51 |

4 NON-LINEAR TIME HISTORY ANALYSIS

4.1 RUAUMOKO3D modelling approach

RUAUMOKO3D was used to conduct non-linear time history analyses of the two buildings designed (Carr, 2004). RC structural walls were modelled as a set of four beam elements. A floor diaphragm constraint was assumed. The mass properties of the systems have been modelled by an additional column containing the lumped storey masses in both translational directions, and a rotational inertia about the vertical axis at each level.

The non-linear behaviour of the wall elements at the base was modelled by plastic hinges. The upper storey wall sections were modelled as elastic elements. The cracked second moment of inertia of each wall was calculated from the moment capacity and yield curvature in line with the recommendations of Priestley et al., (2007). The cracked shear cross-sectional area was found considering the same ratio of the cracked wall section inertia to gross wall section inertia. The 3D building models have been analysed under earthquake excitations in both horizontal directions, neglecting the vertical component. The displacements and hysteretic behaviour for the four-wall structural models were plotted using DYNAPLOT (Carr, 2004). The inter-storey drifts and accelerations obtained with both the non-linear time-history analysis and modal response spectrum analysis were compared to verify the accuracy of the results obtained for 250 and 500 year return periods.

4.2 Ground motions

The non-linear time-history analyses were conducted using a selection of ground motion records collected by Yeow et al., (2018). The ground motion records chosen for the analysis was based on location, fundamental period of vibration in both directions, and soil type. The ground motions assumed were recorded in Wellington, with a spectral acceleration of 0.5 seconds, on a class C subsoil (Yeow et al., 2018). The earthquake database contained nine hazard levels which correspond to a probability of exceedance in 50

years of (1) 80%, (2) 50%, (3) 20%, (4) 10%, (5) 5%, (6) 2%, (7) 1%, (8) 0.5%, and (9) 0.2%, respectively. Each hazard level contained 20 earthquake records, with both the horizontal components.

4.3 Results obtained

The fundamental period of each building was determined with both RUAUMOKO3D and SAP2000. The code-compliant design and LDSD periods with RUAUMOKO3D were found to be 0.56 s and 0.32 s, respectively. These periods closely align with the periods obtained from SAP2000 (Table 4, Table 5). The decreased period of the LDSD reflects an increase in stiffness due to the increase of the wall sections. The maximum inter-storey drifts and accelerations obtained from the non-linear time history analysis of the code-compliant and LDSD buildings are shown in Figure 6 and Figure 7. These figures present the mean results of the 20 earthquake scenarios investigated for each hazard level.

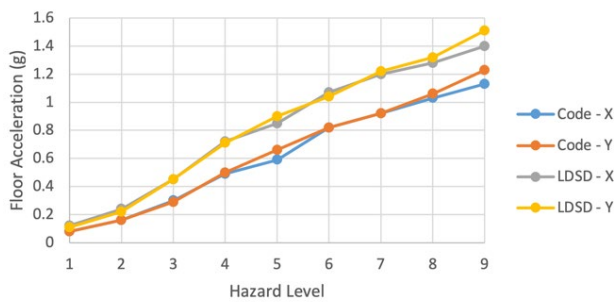


Figure 6. Non-linear time-history floor acceleration for code compliant design and LDSD

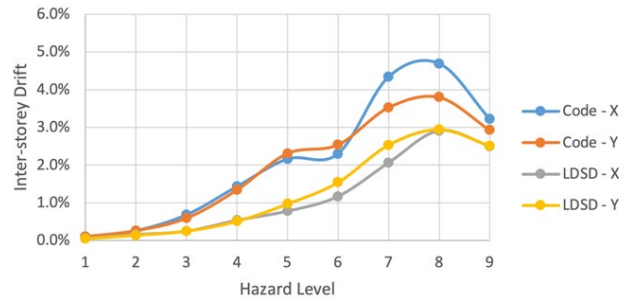


Figure 7. Non-linear time-history inter-storey drift for code compliant design and LDSD

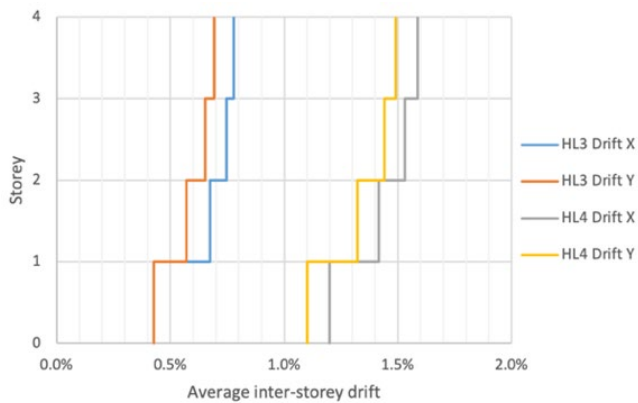


Figure 8: HL3 vs HL4 non-linear time history drift demands for code compliant design

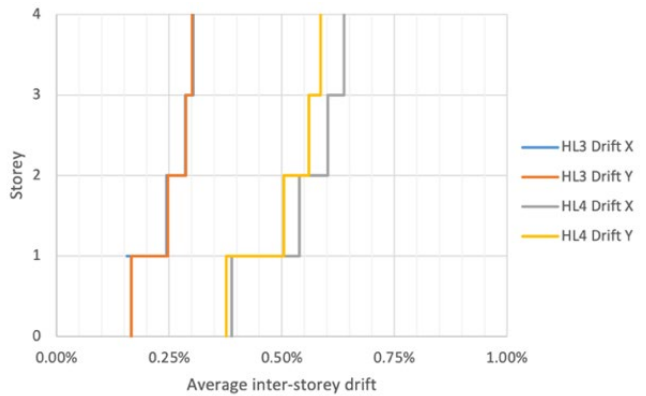


Figure 9: HL3 vs HL4 non-linear time history drift demands for LDSD

The LDSD shows lower inter-storey drift demands and higher accelerations over all hazard levels. The inter-storey drift demands, for the 250-year (HL3) and 500-year (HL4) return periods, show the notable decrease in drift of the LDSD compared to the code-compliant design. The increased wall section of the LDSD system increases the stiffness of the building and a stiffer system generally results in a decrease in drift and increase in floor accelerations. This trend is confirmed by the results presented in Figure 6 and Figure 7. The LDSD wall layout was chosen to minimise torsional effects. The inter-storey drifts for HL3 and HL4 are within the corresponding drift limits as specified by NZS1170.5 and LDSD guidelines (Standards New Zealand, 2004; Campbell, 2018). The reduction of the torsional demand of the LDSD building, compared to the code-compliant building, can be

visualised by observing the decrease of the difference in drift demands between the X and Y directions (Fig. 8-9).

5 LOSS ASSESSMENT

5.1 Overview of loss procedure

The FEMA P-58 PBEE framework has been utilised to examine the difference in cost-effectiveness between designs (Hamburger, 2014). The loss assessment followed the steps of identifying building characteristics, hazard analysis, structural analysis, damage analysis, loss analysis and the decision as specified by PBEE (Deirlein et al., 2003). The guidelines specified in FEMA P-58 Seismic Performance Assessment of Buildings were also considered for the loss assessment process (Hamburger, 2014). The fragility and consequence data calculation tool PACT was used to conduct the loss assessment and compare the expected loss of the code-compliant design to the LDS. The loss assessment was undertaken using probabilistic calculations and accumulation of losses in New Zealand dollars (NZD). The expected annual loss was calculated using the hazard data provided by Yeow et al. (2018).

The loss assessment required a rebuild cost estimate to determine the annual expected costs. The building cost was estimated using a top-down approach. The building construction cost was estimated using data from Rawlinson's construction handbook (Giddens, 2013). The cost per square metre of floor area for the case study building was estimated based on a high quality residential two- or three-bedroom layout with an ensuite from a multi-storey apartment building (including bathroom, WC, laundry, lift to each floor and excluding balcony) (Giddens 2013). An additional 50% increase in cost was considered for the top-level to account for the duplex penthouse layout. The balconies were considered as an additional cost. This top-down estimate gave a total construction estimate of NZD 2,372,400 using data from 2012. Additional GST, professional fees and demolition fees were calculated as a proportion of the construction costs (Table 8). A 24% increase was considered to account for the construction inflation from 2012 to 2020 in the PACT model as a data cost multiplier (Stats New Zealand, 2017).

Table 8: Case study building and rebuild cost estimate.

| Element | Percentage | Cost NZD |
|----------------------|------------|------------------|
| Construction | - | 2,372,400 |
| Professional fees | 11.50% | 272,830 |
| Demo | 15.00% | 396,780 |
| GST | 15.00% | 456,300 |
| Rebuild Total | | 3,498,310 |

The total replacement cost was estimated to be NZD 3,498,000. The building cost was the same for the code design and LDS due to the nature of the top-down approach.

Table 9: PACT performance group components

| | No. | Component type | Source |
|---|------------|---|---------------------|
| Directional (Demand parameter - Storey drift ratio) | B1044.091 | Slender Concrete Wall | PACT |
| | B2011.000 | Exterior glazing partitions | (Yeow et al., 2018) |
| | B2011.001 | Precast cladding panels | (Yeow et al., 2018) |
| | C1011.001a | Wall Partition (gypsum with metal studs) | PACT |
| | C2011.001a | Prefabricated steel stair w/ seismic joints | PACT |
| Non-directional (Demand parameter - Floor acceleration) | C3032.100 | General Suspended Ceilings | PACT |
| | C3033.002 | Recessed lighting in suspended ceiling | PACT |
| | D1014.011 | Traction Elevator | PACT |
| | D2024.000 | Water Pipe System | (Yeow et al., 2018) |
| | D3041.021a | HVAC Stainless Steel Ducting | PACT |
| | D3041.031a | HVAC Drops / Diffusers in suspended ceilings | PACT |
| | D3052.013f | Air Handling Unit (hard anchored or vibration isolated) | PACT |
| | D4011.000 | Fire sprinklers - pipes | (Yeow et al., 2018) |
| | D4011.041a | Fire sprinkler drops | PACT |
| | D5011.013e | Transformer (hard anchored or vibration isolated) | PACT |

5.2 Inventory of damageable components

The damageable building components of the building were determined through a literature review of building loss assessment and the case study architectural layout (Table 9). The components were quantified for PACT for each storey in as X and Y direction components and non-directional components. The damageable components, fragility and loss functions were obtained from two library sources; PACT library and Yeow et al. (2018). Where applicable (and available), seismically restrained components were selected for acceleration-sensitive building components to resist floor acceleration demands as per the low damage guidelines.

5.3 Fragility and loss functions

The damageable components defined for the building generally contain three damage states. The damage states refer to the condition of damageable components after experiencing limit seismic displacement or accelerations. The probability of each damage state is defined by corresponding

fragility and loss functions. The damage fragility functions have a defined average drift or accelerations and an expected repair costs associated with the damage. The fragility and loss functions were used to determine the expected losses for each hazard level which gives a time-based result and an expected annual loss for the building.

5.4 Results obtained

The damageable building components which are critical for the seismic losses change with each hazard level. From the PACT loss assessment analysis, it was found that the partition walls contribute largely to the losses at HL1 to HL3. This shows that the loss at the lower intensities were governed by drift. At HL4, the main contributor to losses remained the partition walls. However, the suspended ceilings and HVAC began to become large contributors to the loss. These two components are acceleration sensitive. These components were major contributors up to HL7. Beyond HL7, the RC walls dominated the loss contribution. The contribution of RC walls increased with hazard level up to HL9. Based on these observations, drift sensitive components contribute to the majority of the expected losses through all hazard levels.

The expected loss of both designs increased with the hazard level, as anticipated. The low damage design has noticeably lower repair costs in lower hazard levels and is most evident in HL3 to HL5 (Fig. 10).

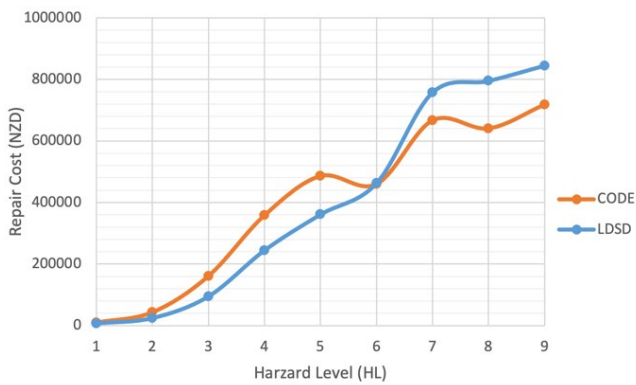


Figure 10: Expected annual repair costs for HL1 to HL9

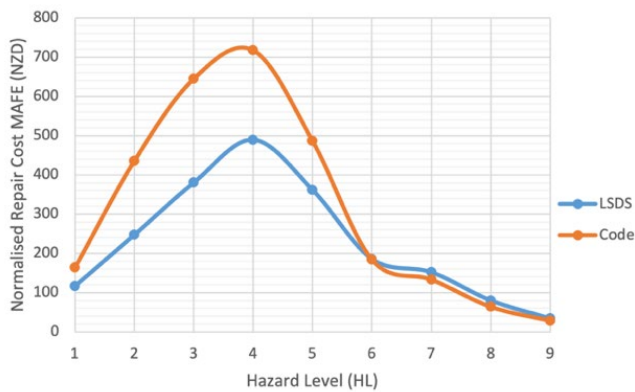


Figure 11: Expected annual repair costs normalised by MAFE for HL1 to HL9

The differences in the repair costs for high hazard levels from HL6 onwards is due to the RC wall damage for the LDS system being less significant but having a larger repair area. Thus, resulting in a larger cost of repair. The dip in losses observed at HL6 is likely due to the variability in the ground motion data.

The normalised loss area chart is based on the mean annual frequency of exceedance (MAFE) (Fig. 11). This considers the repair cost at each hazard-level and the probability of an earthquake of that hazard level occurring. The normalised loss is considerably less for LDS than for code-compliant design for hazard levels up to HL5. The code-compliant design and LDS have negligible differences in normalised damage costs for HL6 to HL9.

The annualized total repair cost for the code-compliant design was determined to be NZD 3157. Figures 12-13 show that less frequent earthquakes (HL1 to HL3) make up the majority of the probabilistic costs. As the expected costs increases, the higher intensity levels make up a larger proportion but with decreased probability.

The relationship of less frequent earthquakes accounting for the majority of the probability at low costs is also apparent for the code-compliant design. The annualized total repair cost for the LDS was determined to be NZD 2197. This 30% decrease in losses indicates that the drift sensitive components of the building contribute to greater losses. This is apparent as the stiffer LDS building has lower drifts but higher floor accelerations

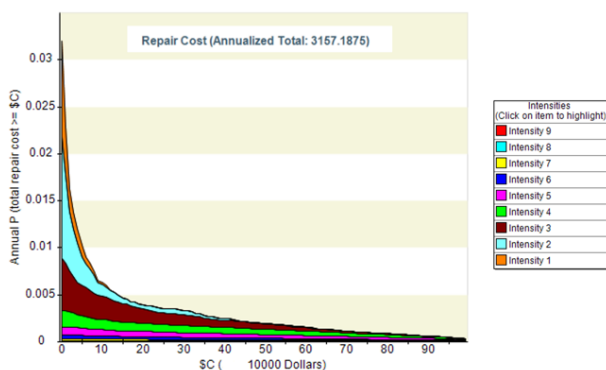


Figure 12: Code compliant design repair costs and annualised total repair costs

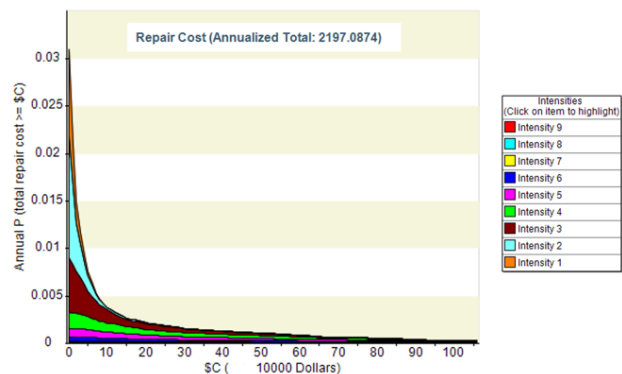


Figure 13: LDS repair costs and annualised total repair costs

Table 10: Expected annual loss for code compliant design and LDSD.

| Design | EAL (NZD) | Ratio of EAL to building replacement cost |
|--------|-----------|---|
| Code | 3157 | 0.090% |
| LDSB | 2197 | 0.063% |

(Table 10).

By undertaking the loss assessment of the code-compliant design and LDSB solution, the LDSB has significantly lower monetary losses. These losses have decreased due to the decreased drift demands and torsional effects on the building. Although the accelerations have increased for each hazard level in the LDSB, the acceleration sensitive losses contribute a significantly smaller proportional of the total loss. Inter-storey drift demands have a larger impact on the overall annual loss of the building as the building components that make the majority of the loss have damage states being dependant on the drift.

6 CONCLUSIONS

This research paper compared the loss estimates obtained for a code compliant and low damage seismic design of a multi-storey medium density residential building. The expected annual losses of the low damage seismic design building were significantly less than the code-compliant design. The expected losses for each hazard level also decreased with low damage seismic design. This was due to the buildings major structure elements damage-states being drift sensitive. As the drift decreased with the low damage seismic design, the damage decreased significantly. This was shown through the 30% reduction in expected annual losses which confidently shows the low damage seismic design has less monetary losses at return periods less than 2500 years (HL6). The monetary losses for return periods greater than 2500 years for the low damage seismic design system increased compared to the code-compliant design. Due to the large return period of 2500 years, the difference in normalised losses between code-compliant design and LDSB are insignificant for the expected annual losses.

It is concluded that the low damage criteria lead to a significant reduction in expected annual losses, and hence improved seismic performance. This improved seismic performance using low damage design criteria will reduce monetary losses and disruption for the stakeholder. It was noted that the major contributors to the loss assessment were drift sensitive. The non-structural drift sensitive elements, such as partition walls, contribute significantly more towards losses at lower and medium hazard levels. The non-structural acceleration sensitive elements contribute more to the expected loss at higher hazard levels. The seismically restrained elements play a large role in minimising acceleration sensitivity. This suggests future research could investigate the effectiveness of using low damage solutions for non- structural elements and evaluate the expected cost- benefit compared to standard non-structural elements.

7 ACKNOWLEDGEMENTS

Acknowledgements to Professor Timothy Sullivan and Giovanni De Francesco for project supervision and research guidance. Acknowledgements to Interspace for architectural drawings for the case study building.

The ratio of expected annual loss to building replacement cost was calculated using the annualised total cost (Fig. 12-13) and the estimated building replacement cost (Table 8). The significantly lower ratio of expected annual loss (EAL) to building replacement cost for the LDSB system shows that low damage design resulted in a significant reduction in losses, and hence improved seismic performance

8 REFERENCES

- Campbell P. (2018). "Proposed Low Damage Design Guideline – A NZ Approach". 17th U.S.- Japan-New Zealand Workshop on the Improvement of Structural Engineering and Resilience, Queenstown, New Zealand, November 12-14.
- Carr, A. (2004). Ruaumoko3D—A program for inelastic time-history analysis, Department of Civil Engineering, University of Canterbury, Canterbury New Zealand.
- Carradine, DM. (2019). Multi-storey Light Timber- Framed Buildings in New Zealand – Engineering Design. BRANZ, Porirua, New Zealand.
- Deirlein, G., Krawinkler, H., and Cornell, C. (2003). "A framework for performance-based earthquake engineering." Proc., 2003 Pacific Conference on Earthquake Engineering, Blume Earthquake Engineering Center, Stanford University, Stanford
- Giddens, C. (2013). Rawlinsons New Zealand Construction Handbook, Rawlinsons Media Limited, Auckland, New Zealand.
- Hamburger, RO. (2014). "FEMA P-58 seismic performance assessment of buildings." Proc., 10th National Conf. in Earthquake Engineering, Earthquake Engineering Research Institute, Anchorage, AK.
- Priestley M.J.N., Calvi, M.C., and Kowalsky, M.J. (2007) Displacement-Based Seismic Design of Structures, IUSS Press, Pavia.
- Standards New Zealand. (2002). 1170.1: 2002— Structural design actions: Part 1: Permanent, imposed and other actions, Standards New Zealand, Wellington, New Zealand.
- Standards New Zealand. (2004a). 1170.5: 2004— Structural Design Actions Part 5: Earthquake actions, Standards New Zealand, Wellington, New Zealand.
- Standards New Zealand. (2004b). 1170.5 Supp1: 2004— Structural Design Actions Part 5: Earthquake actions – New Zealand Commentary, Standards New Zealand, Wellington, New Zealand.
- Standards New Zealand. (2006). 3104: 2006— Concrete structures standard. Standards New Zealand, Wellington, New Zealand.
- Stats New Zealand. (2017). Price indexes for the construction industry, <https://www.stats.govt.nz/methods/price-indexes-for-the-construction-industry> (accessed 1 October 2020).
- Yeow TZ, O. A., Sullivan TJ, MacRae GA, Clifton GC, and Elwood KJ (2018). "Seismic performance of steel friction connections considering direct- repair costs." Bulletin of Earthquake Engineering.